

Original Article



Exposure to Electromagnetic Fields from Mobile Phones and Fructose consumption Coalesce to Perturb Metabolic Regulators AMPK/SIRT1-UCP2/FOXO1 in Growing Rats*

Ruchi Tripathi¹, Sanjay Kumar Banerjee^{2,3}, Jay Prakash Nirala⁴, and Rajani Mathur^{1,#}

1. Department of Pharmacology, Delhi Institute of Pharmaceutical Sciences & Research, Delhi Pharmaceutical Sciences and Research University (DPSR-U), New Delhi, INDIA; 2. Drug Discovery Research Centre, Translational Health Science and Technology Institute, Faridabad, INDIA; 3. Department of Biotechnology, National Institute of Pharmaceutical Education and Research, Guwahati, INDIA; 4. School of Environmental Sciences, Jawaharlal Nehru University, New Delhi, INDIA

Abstract

Objective In this study, the combined effect of two stressors, namely, electromagnetic fields (EMFs) from mobile phones and fructose consumption, on hypothalamic and hepatic master metabolic regulators of the AMPK/SIRT1-UCP2/FOXO1 pathway were elucidated to delineate the underlying molecular mechanisms of insulin resistance.

Methods Weaned Wistar rats (28 days old) were divided into 4 groups: Normal, Exposure Only (ExpO), Fructose Only (FruO), and Exposure and Fructose (EF). Each group was provided standard laboratory chow *ad libitum* for 8 weeks. Additionally, the control groups, namely, the Normal and FruO groups, had unrestricted access to drinking water and fructose solution (15%), respectively. Furthermore, the respective treatment groups, namely, the ExpO and EF groups, received EMF exposure (1,760 MHz, 2 h/day x 8 weeks). In early adulthood, mitochondrial function, insulin receptor signaling, and oxidative stress signals in hypothalamic and hepatic tissues were assessed using western blotting and biochemical analysis.

Result In the hypothalamic tissue of EF, SIRT1, FOXO 1, p-PI3K, p-AKT, Complex III, UCP2, MnSOD, and catalase expressions and OXPHOS and GSH activities were significantly decreased ($P < 0.05$) compared to the Normal, ExpO, and FruO groups. In hepatic tissue of EF, the p-AMPK α , SIRT1, FOXO1, IRS1, p-PI3K, Complex I, II, III, IV, V, UCP2, and MnSOD expressions and the activity of OXPHOS, SOD, catalase, and GSH were significantly reduced compared to the Normal group ($P < 0.05$).

Conclusion The findings suggest that the combination of EMF exposure and fructose consumption during childhood and adolescence in Wistar rats disrupts the closely interlinked and multi-regulated crosstalk of insulin receptor signals, mitochondrial OXPHOS, and the antioxidant defense system in the hypothalamus and liver.

Key words: EMF-mobile phone; Fructose; Childhood-adolescence; Insulin receptor signal; Mitochondrial OXPHOS; Antioxidant system; Hypothalamic insulin resistance; Hepatic insulin resistance

Biomed Environ Sci, 2023; 36(11): 1045-1058

doi: [10.3967/bes2023.134](https://doi.org/10.3967/bes2023.134)

ISSN: 0895-3988

www.besjournal.com (full text)

CN: 11-2816/Q

Copyright ©2023 by China CDC

INTRODUCTION

Insulin resistance (IR) has traditionally been identified as a hallmark characteristic of obesity-associated type 2 diabetes mellitus

(T2DM), wherein the response of peripheral tissues such as the liver, skeletal muscle, and adipose tissue to insulin is reduced. Obesity and IR, which, until recently, were a major concern in adults, have become more prevalent in children and adolescents

*This study was supported by the Indian Council of Medical Research (ICMR) in New Delhi. (Sanction NO:5/10/FR/13/2015-RBMH).

#Correspondence should be addressed to Rajani Mathur, Tel: 91-011-29551490, E-mail: mathurajani@gmail.com

globally. According to the World Health Organization, people who are overweight and obese account for 44% of diabetes cases, 23% of ischemic heart disease cases, and 7%–41% of certain cancers^[1-2]. Per the International Diabetes Federation, diabetes affects 1.1 million children and adolescents aged 14–19 years. In India, the prevalence of prediabetes and diabetes among young adults is 12.3% and 8.4%, respectively. T2DM and IR are strongly linked to obesity, and the prevalence of obesity-related diabetes is expected to double to 300 million by 2025^[3]. The increasing prevalence of IR among children and adolescents is associated with the growing incidence of adult diseases, including T2DM and cardiovascular disease, making it a public health concern^[4].

Recently, the brain was identified as an insulin-responsive organ, and its regulatory role in insulin signaling pathways and glucose metabolism has been established^[5]. IR is a likely pathogenesis of the brain, specifically the hypothalamus (hypothalamic insulin resistance, hyp-IR), a region rich in insulin receptors that may regulate the homeostatic functions of the liver in addition to insulin secretion and its subsequent actions^[6].

Experimental animal studies, epidemiological evidence, and clinical trials have reported that high-fructose corn syrup is singularly responsible for IR development in both adult and pediatric populations^[7-8]. We previously delineated the underlying molecular signals that may mediate the genesis of hepatic IR (hep-IR) in developing rats^[9-11].

Recent trends indicate that modern children and adolescents are increasingly exposed to electromagnetic fields (EMFs) from mobile phones (900–2,000 MHz) during their growth years^[12]. Mobile phones operate on non-ionizing low-frequency EMFs to elicit thermal and non-thermal effects, of which the biological effects have been attributed to the latter^[13-15]. There is particular concern regarding the health effects of mobile phones on children and adolescents, as they are avid, unrestricted, and potential long-term users. Moreover, their developing nervous system, including the brain tissue conductivity and relative head size, makes them more susceptible to highly penetrating EMF radiation^[16].

EMFs from mobile phones can exert nonthermal and thermal effects^[17-18], and the former poses a health risk, thereby making it necessary to define exposure limits. Increasing evidence suggests that non-thermal interactions affect the cardiac, reproductive, and central neurological systems^[19-20].

Non-thermal electromagnetic radiation increases reactive oxygen species (ROS) levels and causes aberrant metabolic activities in biological systems^[21]; however, studies that delineate the underlying molecular mechanism(s) are lacking.

We previously reported that when weaned rats were subjected to concomitant stressors, i.e., EMF radiation from mobile phones (1,760 MHz, 2 h/day) and fructose consumption (15%), the pathways of eating and satiety behaviors that operate to maintain the “set-point” of energy homeostasis in the hypothalamus and liver were severely disturbed by early adulthood^[22]. To the best of our knowledge, this is the first experimental report that implicates these two stressors in the pathogenesis of hyp-IR and hep-IR during growth. The underlying mechanism was postulated to be the disruption of the ghrelin and leptin signaling pathways, which participate in the central neuroendocrine control of energy homeostasis. These stressors shift glucose metabolism towards gluconeogenesis, disrupt insulin signaling, and alter mitochondrial function^[22]. However, there is a paucity of data elucidating the effects of these stressors on the molecular signals of IR, mitochondrial function, and oxidative stress in the hypothalamus and liver of growing rats. This study provides further evidence in continuation of our previous study.

MATERIALS AND METHODS

Animals

Weaned male albino Wistar rats (44.5 ± 10 g; 28 days old) were housed under standard conditions of temperature (22 ± 2 °C), humidity, and dark/light cycle (12/12 h) throughout the experiment. The experiments were conducted in accordance with the guidelines of the Committee for the Purpose of Control and Supervision of Experiments on Animals. All experimental protocols were approved by the Institutional Animal Ethics Committee (IAEC/14/II-04 and DIPSAR/IAEC/15-II/07).

The study duration was 8 weeks, from the weaning day (28 days old) until early adulthood (84 days old), and spanned the pre-, peri-, and post-pubertal stages of rat development. Weaned male Wistar albino rats were randomly divided into four groups ($n = 6$ each), namely: Normal, Exposure Only (ExpO), Fructose Only (FruO), and Exposure with Fructose (EF) for the 8-week study period.

In the Normal group, animals had free access to standard laboratory chow and filtered drinking

water. The animals had free access to standard laboratory chow and 15% fructose as a drinking solution. In the ExpO group, the animals had free access to standard laboratory chow and filtered drinking water. Additionally, they were exposed to EMF from mobile phones (frequency of 1,760 MHz, power density of 0.3988 mW/cm², GSM, and SAR of 0.181 W/kg) for 2 h/day for 8 weeks. In the EF, the animals had free access to standard laboratory chow and 15% fructose as a drinking solution. Additionally, they were exposed to EMF from mobile phones (frequency of 1,760 MHz, power density of 0.3988 mW/cm², GSM, and SAR of 0.181 W/kg) for 2 h/day for 8 weeks.

EMF Exposure

As described earlier, a Plexiglas cage of adjustable length that could comfortably house one rat at a time was used as the exposure chamber^[22]. The mobile phone was placed on top of the exposure chamber such that its antenna preferentially emitted EMF towards the whole body of the rat. The platform carrying the mobile phone was tied firmly with a string to a pulley controlled by a stepper motor (programmed using Pluronic software). The platform was moved using a programmed motor at an angular momentum of 2–45 degrees.

Specific Absorption Rate (SAR) Value

Power was continuously generated using a mobile tower antenna operating at 1.76 GHz continuously. For rats weighing 55–220 g, the whole-body average SAR is 0.18 W/kg.

To measure SAR, the intensity of EMF emitted by the mobile phones was measured with the electric field probe with the transmitter (NADRADH NBM520 Model) operating at a frequency range of 1.76–1.92 GHz and ensured that exposure from EMF radiation was evenly distributed on rat. The average power density in the range of 0.0968–0.3988 mW/cm² was used to measure the SAR value against whole body weight (g), length (from head to tail tip) (cm), and width (cm) of the exposed rats every week of the study period.

Using this system, the ExpO and EF groups received EMF exposure from mobile phones in “switched-on mode” (1,760 MHz, 0.3988 mW/cm², specific absorption rate 0.181 W/kg, 2 h/day x 8 weeks)

Sample Collection

After the study period ended, the rats were euthanized using CO₂ to surgically remove the

hypothalamus and liver that were immediately stored (–80 °C), as detailed elsewhere^[22].

Western Blotting

The hypothalamic and hepatic tissue samples were homogenized in 0.1% RIPA lysis buffer with 100 µL protease inhibitor and centrifuged (13,000 ×g, 15 min, 4 °C), after which the protein content was measured^[23]. The samples were denatured in a sample-reducing buffer (Pierce™ lane marker reducing sample buffer, Cat #39000, Thermo Scientific, USA), and proteins (20 µg/lane) were resolved on a 10% SDS-polyacrylamide gel by electrophoresis and then transferred to nitrocellulose membrane (90 min at 90 V, Bio-Rad system, USA). The blots were incubated with a blocking buffer (3% BSA) in Tris-buffered saline containing 0.2% Tween 20 (TBS-T) for 1 h at room temperature followed by overnight incubation (4 °C) with the primary antibodies: anti-p-AMPKα (Thr 172) (1:500; Cat #40H9, Cell Signaling Technology, USA), anti-SIRT 1 (1:1,000; Cat #9475, Cell signaling Technology, USA), anti-UCP2 (1:1,000; Cat #NBP100-59742, Novus biological, USA), anti-IRS1 (1:1,000; Cat #59G8, Cell signaling Technology, USA), anti-AKT (1:1,000; Cat #9272, Cell signaling Technology, USA), anti-p-AKT (1:1,000; Cat #Ser 473, Cell signaling Technology, USA), anti-p-PI3K (1:1,000; Cat #bs-3332-R, Bioss, USA), anti-FOXO 1 (1:500; Cat #D7C1H, Cell signaling Technology USA), anti-OXPHOS (Cocktail of Complex I, II, III, IV and V) (1:500; Cat #ab110413, Abcam, USA), anti-MnSOD (1:1,000; Cat #14C10, Cell signaling Technology, USA), anti-Catalase (1:1,000; Cat #ab52477, Abcam, USA), and anti-GAPDH (1:1,000; Cat #14C10, Cell Signaling Technology, USA). The blots were then washed thrice with TBS-T and incubated with secondary anti-rabbit/ anti-mouse or IgG-HRP antibody (1:10,000, Cat #ab97051, Abcam Sigma Aldrich, St. Louis, Missouri, USA), and immunodetection was performed using enhanced chemiluminescence (Luminata strong™-Western HRP substrate, Merck-Millipore, Billerica, MA, USA) and quantified (Gel ChemiDoc™, Bio-Rad imaging system, USA). Digital images were analyzed by densitometry using the ImageJ software (National Institutes of Health, Bethesda, MD, USA).

Determination of Oxidative Stress Markers Activity

Superoxide Dismutase Frozen hypothalamic (50 mg) and liver (100 mg) tissues were thawed, homogenized in phosphate-buffered saline (0.1 mol/L, pH 7.4), and centrifuged (10,000 rpm,

5 min, 4 °C). Superoxide dismutase (SOD) activity in the supernatant was determined as the amount of enzyme required for 50% inhibition of pyrogallol autoxidation per mL of assay mixture and was expressed as U/(min·mg) protein. The assay mixture contained freshly prepared pyrogallol (100 µL, 0.13 mmol/L), HCl (10 mmol/L), and EDTA (3.3 mmol/L). The reaction was initiated by the addition of pyrogallol (100 µL) in the supernatant sample (100 µL) and the rate of increase in the absorbance at 420 nm was recorded spectrophotometrically for 2 min (from 1 min 30 s to 3 min 30 s, Aqua Mate AQ 8000, Thermo Scientific, USA). A lag time of 1 min 30 s was allowed to attain a steady state for pyrogallol autoxidation^[24].

Catalase Frozen hypothalamus (50 mg) and liver (100 mg) were thawed, homogenized with potassium phosphate buffer (50 mmol/L, pH 7.4), and centrifuged (3,400 rpm, 15 min, 4 °C)^[25]. The supernatant was analyzed for catalase activity based on the formation of chromic acetate from dichromate and glacial acetic acid using hydrogen peroxide^[26]. The assay mixture contained H₂O₂ solution (400 µL, 0.8 mmol/L), phosphate buffer (500 µL, 50 mmol/L, pH 7.0), and supernatant sample (100 µL). The assay mixture (1 mL) was added to the dichromate/acetate solution at 60-s intervals. The solution was placed in a water bath (100 °C, 10 min) until a stable green color developed, which was determined spectrophotometrically at 570 nm. The catalase activity was expressed as µmol H₂O₂ consumed per 30 s per mg protein.

Reduced Glutathione Frozen hypothalamus (50 mg) and liver tissue (100 mg) were thawed, homogenized in phosphate buffer saline (500 µL, 0.1 mol/L, pH 7.4), centrifuged (10,000 rpm, 5 min, 4 °C), and analyzed.

Reduced glutathione (GSH) was directly determined by the oxidation of 5,5'-dithiobis (2-nitrobenzoic acid) to 5-thio-2-nitrobenzoic acid. The tissue homogenate (0.5 mL) was precipitated with 5% TCA (2 mL) containing EDTA (1 mmol/L) and centrifuged (200 rpm, 10 min). The reaction mixture contained freshly prepared Ellman's reagent (2,2'-dinitro-5,5'-dithiobenzoic acid) phosphate buffer (0.3 mol/L), 1% sodium citrate (1.8 mL, 0.1 mmol/L), and supernatant sample (0.2 mL). The reaction mixture was incubated at 30 °C for 10 min and the change in absorbance per minute was recorded at 412 nm. The GSH content was expressed as µmol/mg wet tissue^[27].

Isolation of Mitochondrial Enriched Fraction

Hypothalamus The frozen hypothalamus was

thawed, washed, minced, and homogenized in mitochondria isolation buffer containing Tris-HCl (50 mmol/L), NaCl (120 mmol/L), KCl (5 mmol/L), MgSO₄ (1 mmol/L), CaCl₂ (1 mmol/L), glycerol (10%), sucrose (1 mol/L), protease inhibitor (1:100 of buffer), and pH 7.4 using homogenizer (3 strokes, 1 min). The homogenate was centrifuged (600 ×g, 10 min, 4 °C) twice, and the obtained supernatant was re-centrifuged (13,000 ×g, 5 min, 4 °C) to precipitate mitochondrial enriched fraction^[28]. Samples of the mitochondria-enriched fraction were assayed for protein concentration^[29].

Liver buffer containing Tris-HCl (50 mmol/L), NaCl (120 mmol/L), KCl (5 mmol/L), MgSO₄ (1 mmol/L), CaCl₂ (1 mmol/L), glycerol (10%), sucrose (1 mol/L), protease inhibitor (1:100 of buffer); pH 7.4 using homogenizer (10 strokes, 1 min). The homogenates were centrifuged (740 ×g, 5 min, 4 °C) and the supernatant was re-centrifuged (9,000 ×g, 10 min, 4 °C). The supernatant was centrifuged (10,000 ×g, 10 min, 4 °C) to precipitate the mitochondrial fraction^[30]. The pellets were collected, resuspended in (1.5 mL) mitochondrial suspension medium, and assayed for protein concentration using the Bradford method^[29].

Determination of Mitochondrial Respiratory Chain (Oxidative Phosphorylation)–Enzyme Activity

NADH-ubiquinone Oxidoreductase (Complex I Activity) The activity of Complex I was determined as the rate of reduction of dichlorophenolindophenol (DCPIP) to oxidized NADH. The reaction mixture (950 µL) contained monobasic potassium phosphate (25.0 mmol/L), dichlorophenolindophenol (50.0 mmol/L), antimycin A (1.0 mmol/L), decylubiquinone (17.5 mmol/L), (5.0 mg/mL), BSA, and mitochondrial enriched sample (50.0 µL, approximately 30.0 µg). The reaction mixture was allowed to equilibrate (RT, 1 min), and the reaction was initiated with NADH (20.0 µL, 0.8 mmol/L) and rotenone (4.0 µmol/L) and monitored every 30 s for 3 min^[31]. Absorbance was recorded at 600 nm. Enzyme activity was expressed as nanomoles of NADH-reduced/min/mg protein^[32].

Succinate-ubiquinone Oxidoreductase (Complex II Activity) The reaction mixture with a mitochondrial-rich fraction (50 µL), DCPIP (80 mol/L), succinate (10 mmol/L), rotenone (4 µmol/L), and ATP (0.2 mmol/L) was incubated (10 min, 30 °C), and the reaction was initiated with decylubiquinone (80 µmol/L). Enzyme activity was monitored as the decrease in absorbance at 600 nm for 5 min. Malonate (10 mmol/L), which is a competitive

inhibitor, was added to inhibit succinate^[33]. Succinate decylbiquinone reductase activity was expressed as nmol/L 2,6-dichlorophenolindophenol (DCPIP) reduced/min/mg protein.

Cytochrome C Oxidase (Complex IV Activity)

Cytochrome c activity was determined by measuring the oxidation of reduced cytochrome c using dithiothreitol. The reaction mixture contained reduced cytochrome C (0.1 mL) and a mitochondrial-rich fraction sample (50 μ L). The decrease in absorbance was measured at 550 nm (3 min) as the rate of disappearance of reduced cytochrome C^[34]. Enzyme activity was expressed as nanomoles of cytochrome c oxidized/min/mg protein.

ATPase Synthase (Complex V Activity)

ATPase activity was measured directly by measuring inorganic phosphate release from ATP. The reaction mixture contained oligomycin (2 mmol/L), MgCl₂ (50 mmol/L), EDTA (0.2 mmol/L), and Tris-HCl (50 mmol/L, pH 8). A mitochondrial-rich fraction sample (50 μ L) was pre-incubated (10 min), and ATP (5 mmol/L) was added^[35]. The reaction was terminated after 5 min using 10% (w/v) trichloroacetic acid. After centrifugation (800 g, 5 min), the phosphorus content in the clear supernatant was measured at 680 nm^[36].

Statistical Analysis Statistical analysis was performed with a two-way analysis of variance (ANOVA) followed by the Bonferroni post hoc test using GraphPad Prism ver. 5.0. (San Diego, CA, USA). For each analysis, the values are represented as Mean \pm SD ($n = 6$). A value of * $P < 0.05$ vs. Normal, ^S $P < 0.05$ vs. ExpO, [#] $P < 0.05$ vs. FruO and ^o $P < 0.05$ vs. ExpO was considered statistically significant.

RESULT

Effect of EMF from Mobile Phone and Fructose Consumption on Hypothalamic Master Metabolic Regulators (AMPK, SIRT-1, FOXO-1), Insulin Signaling (IRS-PI3K/AKT) Pathway, OXPHOS, and Antioxidant Defense System

AMPK plays key roles as an energy sensor, a metabolic regulator, and a mitochondrial function and homeostasis regulator. The hypothalamic expression of intracellular energy sensor p-AMP-activated protein kinase (p-AMPK α) normalized with respect to internal loading control in Normal, ExpO, FruO, and EF was 1.04 ± 0.24 , 1.24 ± 0.66 , 1.16 ± 0.67 , and 1.05 ± 0.05 , respectively (Figure 1A).

SIRT1 is a sirtuin deacetylase target protein that regulates energy balance aspects *via* mitochondrial

OXPHOS. It functions as a sensor of redox changes and as a master metabolic mitochondrial homeostasis regulator. The master metabolic regulator of mitochondrial homeostasis, sirtuin 1 (SIRT1), normalized to GAPDH, was significantly reduced ($P < 0.05$) in ExpO, FruO, and EF compared to normal. EF also showed a significant ($P < 0.05$) reduction in SIRT1 expression compared to ExpO and FruO (Figure 1B), suggesting that AMPK-dependent SIRT 1 activity was reduced, which may have disrupted the mitochondrial redox equilibrium for ROS generation mediated by uncoupling protein (UCP2).

The hypothalamic insulin transcription factor and mitochondrial oxidative stress regulator, FOXO-1 normalized to GAPDH, were markedly reduced ($P < 0.05$) in FruO and EF compared to the Normal group. Moreover, FOXO-1 expression in EF was significantly ($P < 0.05$) lower than that in the ExpOs group (Figure 1C) which may have disturbed mitochondrial function *via* mitochondrial OXPHOS and insulin signaling.

The hypothalamic expression of the key target, insulin receptor tyrosine kinase protein (IRS1), was significantly lower ($P < 0.05$) in the ExpO and FruO groups than in the Normal group (Figure 1D). Intracellular insulin signal transducer protein (p-PI3K) was significantly decreased ($P < 0.05$) in the ExpO and EF groups. FruO showed significantly lower ($P < 0.05$) p-PI3K expression compared to the ExpO group (Figure 1E). Intracellular insulin signal transducer protein B (p-AKT) was significantly reduced ($P < 0.05$) in the ExpO, FruO, and EF groups compared to the Normal group. p-AKT expression was also reduced in the EF group compared to the FruO group. (Figure 1F). Hypothalamic expression of AKT normalized to GAPDH was significantly decreased ($P < 0.05$) in ExpO and FruO mice compared to normal mice. However, EF showed a significant increase ($P < 0.05$) in AKT expression compared to the ExpO group (Figure 1G). These results indicate that the reduced expression of IRS1, PI3K, and AKT in the hypothalamus impairs insulin signaling, leading to hypothalamic IR.

The hypothalamic protein expression of the mitochondrial OXPHOS, and complex-III in the Normal, ExpO, FruO, and EF groups was 1.56 ± 0.809 , 1.793 ± 0.524 , 1.82 ± 0.178 , and 1.34 ± 0.916 , respectively and was significantly reduced ($P < 0.05$) in FruO and EF than in Normal (Figure 2A). Complex IV expression was 2.12 ± 0.618 , 1.37 ± 0.33 , 0.92 ± 0.43 , and 1.12 ± 0.92 in the Normal, ExpO, FruO, and EF groups, respectively, and was significantly

reduced ($P < 0.05$) in FruO than in Normal (Figure 2B). The hypothalamic complex V expression in the Normal, ExpO, FruO, and EF groups was 1.57 ± 0.34 , 1.95 ± 0.28 , 1.93 ± 0.11 , and 1.22 ± 0.5 , respectively (Figure 2C).

The activity of the hypothalamic mitochondrial OXPHOS enzyme NADH CoQ reductase (complex I) was significantly lower ($P < 0.05$) in the FruO and EF groups than in the Normal group. Also, the Complex I activity was significantly decreased ($P < 0.05$) in the EF group compared to that in the ExpO group (Figure 2D). The succinate-ubiquinone oxidoreductase (complex II) level in the Normal, ExpO, FruO, and EF groups was 0.034 ± 0.004 , 0.034 ± 0.001 , 0.031 ± 0.007 , and 0.015 ± 0.006 nmol/L, respectively. It was significantly reduced ($P < 0.05$) in EF compared to that in the Normal, ExpO,

and FruO groups (Figure 2E).

The cytochrome C oxidase (complex IV) level in the Normal, ExpO, FruO, and EF groups was 1.121 ± 0.15 , 0.76 ± 0.27 , 0.92 ± 0.08 , and 0.28 ± 0.15 nmol/L, respectively. It was significantly reduced ($P < 0.05$) in the EF group compared to that in the Normal, ExpO, and FruO groups (Figure 2F). Moreover, the complex II and complex IV activities in EF were significantly lower ($P < 0.05$) than those in the ExpO and FruO groups. The hypothalamic ATP synthase (Complex-V) activity significantly decreased ($P < 0.05$) in the ExpO, FruO, and EF groups compared to that in the Normal group. Complex V activity was also significantly decreased ($P < 0.05$) in the EF compared to the ExpO and FruO groups (Figure 2G). Taken together, the reduced hypothalamic OXPHOS in the EF evidences

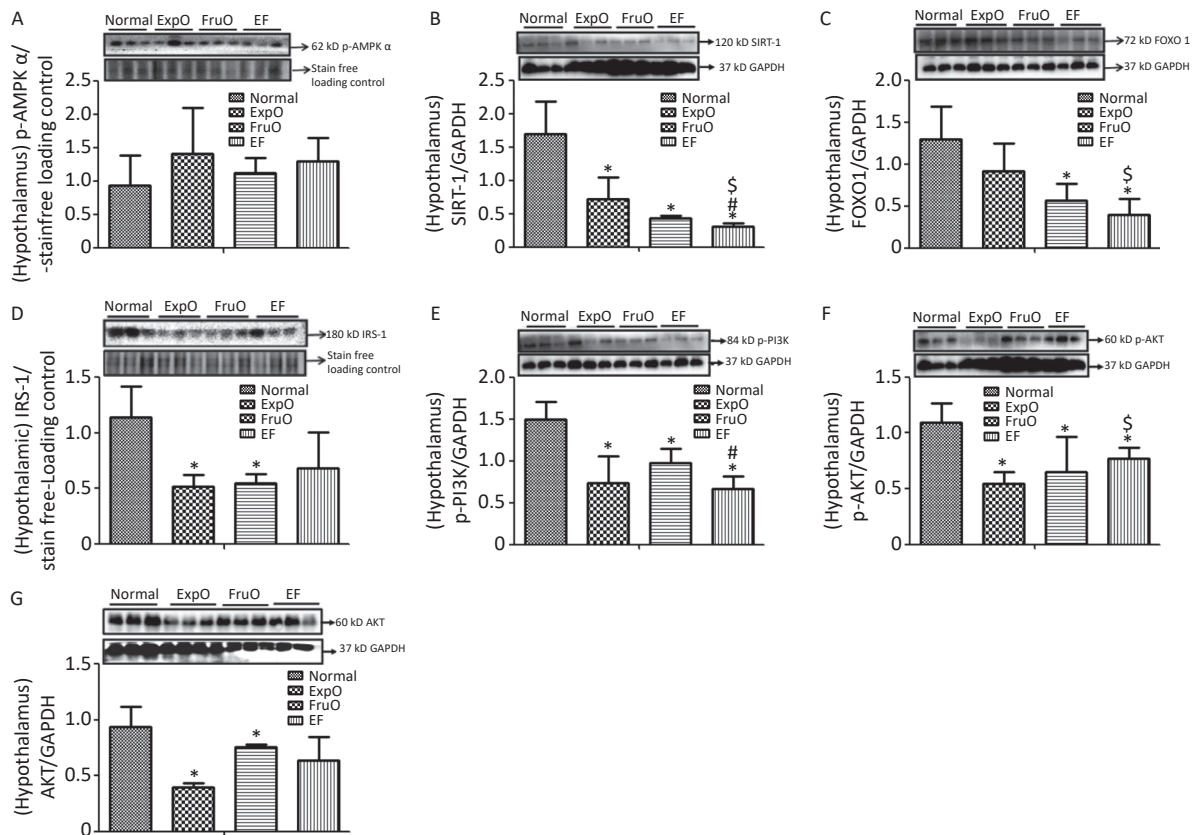


Figure 1. Effect of EMF and fructose consumption in childhood-adolescence perturbed the hypothalamic master regulator protein of mitochondrial and insulin functions and skews hypothalamic transmitting insulin signaling *via* PI3K/AKT by early adulthood. (A) Metabolic key regulator protein p-AMPK α remained unaffected in EF, and (B) SIRT1 was significantly reduced in EF. (C) Expression of the insulin function regulator protein-FOXO-1 was markedly reduced in EF. (D) Hypothalamic expression of signaling adapter protein IRS1 was significantly reduced in ExpO and FruO. (E) Transducer protein PI3K expression was significantly reduced in EF. (F) Expression of the protein p-AKT was significantly reduced in EF and (G) AKT was unchanged. Thus, this shows hypothalamic PI3K/AKT signaling is impaired to attenuate the insulin signaling in response to glucose metabolism and energy regulation.

mitochondrial dysfunction therein and may be responsible for hyp-IR.

UCP2 is located in inner mitochondria and regulates mitochondrial ROS production. Here, we

report that its hypothalamic expression, normalized against that of the internal loading control, was significantly reduced ($P < 0.05$) in FruO and EF compared to the Normal group. Additionally, UCP2

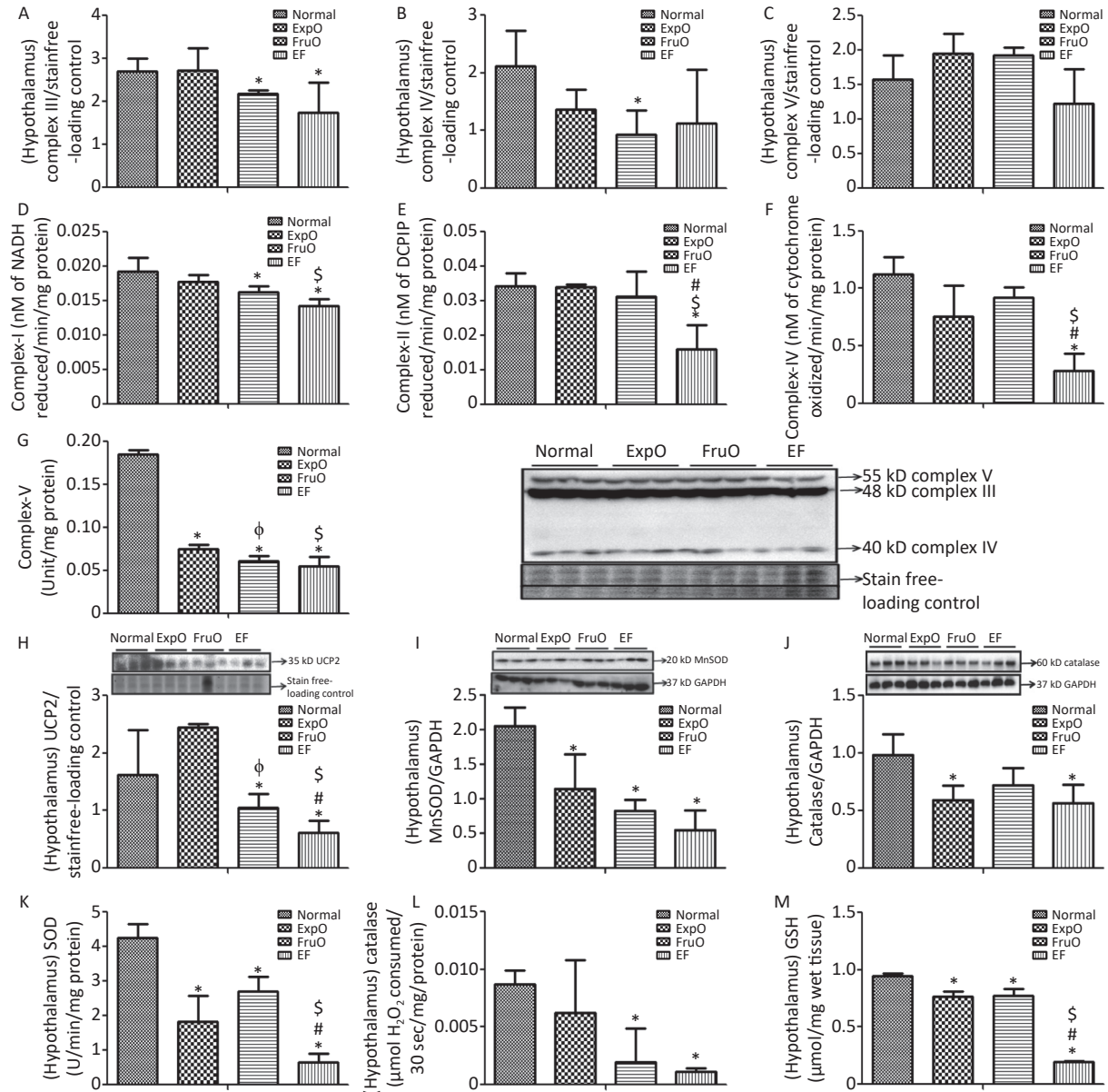


Figure 2. Effect of EMF and fructose consumption in childhood-adolescence interrupt hypothalamic mitochondrial oxidative phosphorylation (OXPHOS) system in ATP production and skews antioxidant defensive system by early adulthood. (A) Hypothalamic expression of Complex III was significantly reduced in EF. (B) and (C) Expression of protein Complex IV was significantly reduced in FruO and Complex V was unchanged in EF. (D) The activity of Complex I was significantly reduced in EF. (E, F, and G) Activity of Complex II, Complex IV, and Complex V was markedly reduced in EF. (H) Hypothalamic UCP2 expression, an ROS regulator, was significantly reduced in EF. (I) Expression of MnSOD, a ROS regulator, was significantly reduced in EF. (J) Expression of Catalase, which protects from ROS-induced oxidative damage, was significantly reduced in EF. (K, L, and M) Activity of SOD, catalase, and GSH was significantly reduced in EF.

expression was significantly reduced ($P < 0.05$) in FruO and EF compared to that in ExpO (Figure 2H). The expression of the hypothalamic mitochondrial protein, manganese-dependent superoxide dismutase (MnSOD), was markedly reduced ($P < 0.05$) in the ExpO, FruO, and EF groups compared to the Normal group (Figure 2I). The hypothalamic expression of the protein catalase normalized against GAPDH was significantly decreased ($P < 0.05$) in the ExpO and EF groups compared to the Normal group (Figure 2J).

The hypothalamic level of antioxidant enzymes SOD in the Normal, ExpO, FruO, and EF groups was 4.26 ± 0.38 , 1.82 ± 0.75 , 2.71 ± 0.42 , and 0.66 ± 0.23 U, respectively, and was significantly reduced ($P < 0.05$) in the ExpO, FruO, and EF groups compared to the Normal group. SOD activity in the EF group was significantly lower ($P < 0.05$) than that in the ExpO and FruO groups (Figure 2K). Hypothalamic catalase activity was significantly reduced ($P < 0.05$) in the FruO and EF groups compared to that in the Normal group (Figure 2L). The hypothalamic activity of GSH in the Normal, ExpO, FruO, and EF groups was 0.94 ± 0.03 , 0.76 ± 0.046 , 0.77 ± 0.05 and 0.19 ± 0.01 U, respectively, and was significantly reduced ($P < 0.05$) in the ExpO, FruO, and EF groups compared to the Normal group. Furthermore, EF significantly reduced ($P < 0.05$) GSH activity compared to ExpO and FruO (Figure 2M). The results indicated that the combined effects of exposure to EMF from mobile phones and fructose consumption severely disturbed the ROS regulator protein, leading to disruption of the activities of the antioxidant enzymes in EF.

Effect of EMF from Mobile Phone and Fructose Consumption on Hepatic Master Metabolic Regulators (AMPK, SIRT 1, FOXO 1), Insulin Signaling (IRS-PI3K/AKT) Pathway, OXPHOS, and Antioxidant Defense System

The hepatic expression of the protein p-AMPK- α was significantly increased ($P < 0.05$) in EF as compared to the Normal, ExpO, and FruO groups. Additionally, the hepatic p-AMPK- α expression was significantly reduced ($P < 0.05$) in the EF group compared to the ExpO group (Figure 3A). The expression of hepatic SIRT1 normalized against GAPDH was significantly reduced ($P < 0.05$) in FruO and EF compared to the Normal group. Hepatic SIRT1 expression in the EF and FruO groups was significantly reduced ($P < 0.05$) compared to the ExpO group (Figure 3B). The expression of the transcription factor FOXO1 normalized to GAPDH

was significantly decreased ($P < 0.05$) in FruO and EF compared to normal (Figure 3C). A reduction in the levels of master metabolic regulators, as observed in EF, has been implicated in the disruption of insulin signaling and mitochondrial function, which may lead to the pathogenesis of hep-IR.

Hepatic expression of the insulin receptor tyrosine kinase protein (IRS1) and intracellular signal transducer, p-PI3K, normalized to GAPDH, was significantly reduced ($P < 0.05$) in the FruO and EF groups compared to the Normal group. The expression of p-PI3K was significantly reduced ($P < 0.05$) in FruO and EF compared to that in ExpO (Figure 3D–E). The expression of hepatic p-AKT normalized to GAPDH was significantly lower ($P < 0.05$) in ExpO and FruO cells, whereas AKT expression remained unchanged (Figure 3F–G).

The expression of hepatic OXPHOS proteins, Complex II (Succinate-Ubiquinone Oxidoreductase), Complex III (Ubiquinol-Cytochrome C Oxidoreductase) was significantly reduced ($P < 0.05$) in ExpO, FruO, and EF than Normal (Figure 4A–B). Hepatic expression of Complex IV (Cytochrome C Oxidase) and Complex V (ATP synthase) was significantly reduced ($P < 0.05$) in the EF group compared to that in the Normal group (Figure 4C–D).

The hepatic OXPHOS enzyme NADH CoQ reductase (Complex I) activity was significantly lower ($P < 0.05$) in the ExpO, FruO, and EF groups than in the Normal (Figure 4E). Succinate-ubiquinone oxidoreductase (Complex-II) activity in the Normal, ExpO, FruO, and EF groups was 0.021 ± 0.004 , 0.013 ± 0.003 , 0.009 ± 0.002 , and 0.004 ± 0.002 nmol/L, respectively and significantly reduced ($P < 0.05$) in the ExpO, FruO and EF groups compared to the Normal groups. A significant decrease ($P < 0.05$) in the activity of Complex IV in FruO and EF was recorded compared to that in ExpO (Figure 4F). The activity of cytochrome C oxidase (Complex IV) in Normal, ExpO, FruO, and EF was 3.02 ± 0.91 , 1.05 ± 0.21 , 1.47 ± 0.24 , and 0.46 ± 0.07 nmol/L, respectively. Complex IV activity was significantly reduced ($P < 0.05$) in ExpO, FruO, and EF compared to Normal; FruO and EF also showed a significant decrease ($P < 0.05$) in the activity of Complex IV compared to ExpO (Figure 4G). The hepatic ATP synthase (Complex V) activity was significantly reduced ($P < 0.05$) in the ExpO and FruO groups compared to the Normal group. However, EF showed a significant decrease ($P < 0.05$) in Complex V activity compared to Normal, ExpO, and FruO. (Figure 4H). Taken together, the reduced hepatic OXPHOS activity in EF may be associated with

mitochondrial dysfunction, leading to hep-IR.

The hepatic mitochondrial uncoupling protein (UCP2) expression was significantly decreased ($P < 0.05$) in the EF group compared to the Normal, ExpO, and FruO groups (Figure 4I). The hepatic expression of the proteins manganese superoxide dismutase (MnSOD) normalized with GAPDH was significantly reduced ($P < 0.05$) in the ExpO, FruO, and EF groups compared to the Normal group. EF showed a significant decrease ($P < 0.05$) in MnSOD expression compared to FruO (Figure 4J). The expression of hepatic catalase normalized to that of GAPDH remained unaffected in the EF (Figure 4K). The level of hepatic SOD enzyme in the Normal, ExpO, FruO, and EF groups was 0.003 ± 0.0003 , 0.002 ± 0.0002 , 0.007 ± 0.0002 , and 0.0018 ± 0.0001 U, respectively,

and significantly decreased ($P < 0.05$) in ExpO, FruO, and EF than Normal. SOD activity was significantly lower ($P < 0.05$) in the EF group than in the ExpO group (Figure 4L). Hepatic catalase and GSH levels were significantly lower ($P < 0.05$) in the ExpO, FruO, and EF groups than in the Normal group (Figure 4M–N). The results indicated that the combined effect of ELF exposure and fructose consumption during childhood and adolescence severely decreased the mechanisms of antioxidant activity in EF.

DISCUSSION

The hypothalamus mediates two important and interlinked roles *via* insulin: food intake and hexose

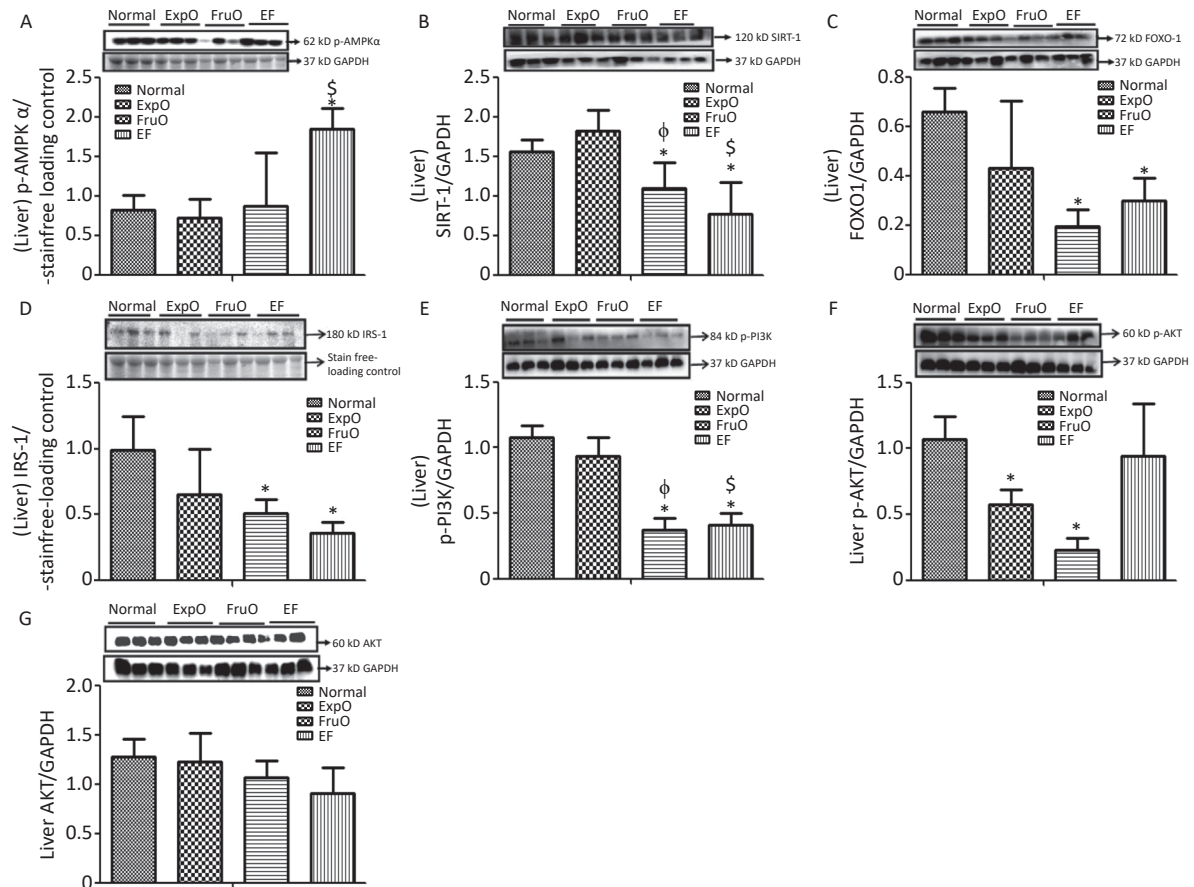


Figure 3. Effects of EMF and fructose consumption during childhood and adolescence on hepatic master regulator proteins of mitochondrial and insulin function and impairment of hepatic insulin signaling *via* PI3K/AKT in early adulthood. (A) Metabolic key regulator protein p-AMPK α was significantly increased in EF and (B) SIRT1 was significantly reduced in EF. (C) Expression of the transcription factor mediator of insulin function and mitochondrial OXPHOS. FOXO-1 was markedly reduced in EF. (D) Hepatic signaling adapter protein IRS1 was significantly reduced in FruO and EF. (E) Expression of transducer protein p-PI3K was significantly reduced in FruO and EF. (F) Expression of the protein p-AKT was significantly reduced in ExpO and FruO. (G) AKT was unchanged in EF.

metabolism regulation. The disruptive state of these two central functions is identified as hyp-IR, for

which factors such as stress, inflammation, and a high-fat diet are implicated; however, the exact

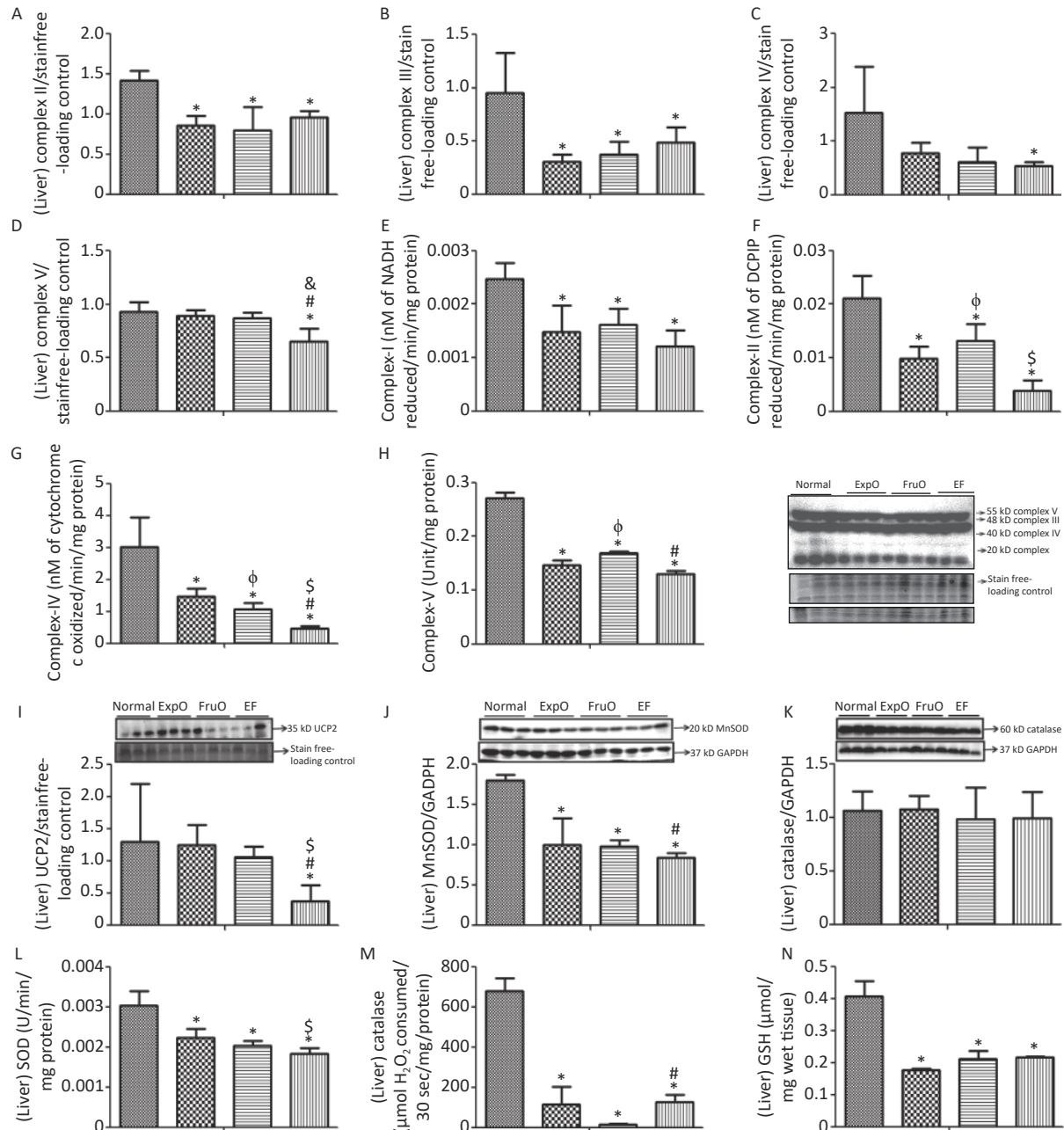


Figure 4. Effect of EMF and fructose consumption in childhood-adolescence interrupt hepatic mitochondrial oxidative phosphorylation (OXPHOS) Complex (I–V) in ATP production and skews the hepatic antioxidant defensive system by early adulthood. (A–B) Hepatic expression of Complex II and Complex III was significantly reduced in ExpO, FruO, and EF. (C–D) Expression of protein Complex IV and Complex V was significantly reduced in EF. (E, F, G, and H) Activity of Complex I, Complex II, Complex IV, and Complex V was markedly reduced in EF. (E) Hepatic expression of UCP2, a ROS regulator, was significantly reduced in EF (I) Expression of MnSOD, a ROS regulator, was significantly reduced in ExpO, FruO, and EF. (J) Expression of Catalase, which protects from ROS-induced oxidative damage, was significantly unchanged in EF. (K) Expression of Catalase was significantly reduced in EF. (L, M, and N) Activity of SOD, catalase, and GSH was significantly reduced in EF.

etiology remains unknown^[37]. The liver is responsible for insulin-mediated glucose uptake, gluconeogenesis suppression, and lipolysis, and the disruption of these actions leads to the pathogenesis of hep-IR^[38]. The hallmark of hep-IR is the dysregulation of two key gluconeogenic enzymes, phosphoenolpyruvate carboxykinase and glucose-6 phosphatase^[39]. Thus, hyp-IR and hep-IR are characterized by altered insulin signaling that manifests as skewed food intake, hexose metabolism, and obesity, which are global health concerns^[37].

Excess fructose consumption is believed to be a major contributing factor to chronic metabolic diseases, including IR, hypertriglyceridemia, nonalcoholic fatty liver disease, hyperglycemia, T2DM, obesity, and cancer^[40]. According to data from the National Health and Nutrition Examination Survey, children aged 2–18 years derive 40% of their total energy from solid fats and added sugars present in soda, fruit drinks, dairy desserts, grain desserts, and pizza^[41]. Consumption of high-fructose corn syrup has increased over the last 10–20 years, particularly among children and adolescents^[42-45]. This increase has been associated with the emergence of IR, obesity, and metabolic problems in developing age groups.

We previously reported that weaned rats provided access to fructose solution (15%) for 8 weeks exhibited increased fasting blood glucose, decreased hepatic hexokinase, and decreased glucose tolerance by early adulthood^[9]. Downregulation of intracellular signals such as PI3K/AKT and JAK-STAT3 has emerged as molecular evidence for IR development in early adulthood^[9-11]. Here, we add to this knowledge by demonstrating the combined effects of two stressors [EMF from mobile phone (2 h/day) and unrestricted fructose (15%) consumption] during the pre-, peri-, and post-pubertal stages of development in the early pathogenesis of hyp-IR and hep-IR.

It has been established that the hypothalamus and liver communicate with each other *via* neuropeptides such as leptin, ghrelin, and NPY to regulate food intake, satiety, and energy expenditure, and the disruption of this pathway leads to the pathogenesis of IR^[46-47]. In the present study, hypothalamic expression of AMPK and NPY was diminished in EF mice by early adulthood. This explains the imbalanced feeding behavior, metabolism, and insulin signaling in EF mice.

In the hypothalamus, the IRS1/PI3K/AKT is the dominant regulatory molecular pathway involved in

hexose metabolism^[48]. Here, for the first time, we provide crucial experimental data showing that central and peripheral master metabolic regulators (AMPK-SIRT1/UCP2-FOXO1), insulin receptor substrate signals (IRS1/PI3K/AKT), and mitochondrial function (OXPHOS) are severely disrupted in the pathogenesis of hyp-IR and hep-IR. These results, in conjunction with our previous data, explain the global epidemic of hyp-IR and hep-IR in children, adolescents, and young adults to a considerable extent^[22].

Previous studies have shown that low ATP levels activate the energy sensor protein AMPK, which restores cellular ATP reserves *via* fatty acid oxidation^[49-50]. We previously reported that AMPK expression is reduced in EF compared to the Normal group^[22]. Here, we show here that in EF mice, mitochondrial oxidative phosphorylation and IRS may explain the shift in metabolism from glycolysis to gluconeogenesis.

SIRT1 is a sirtuin deacetylase target protein that regulates energy balance *via* mitochondrial OXPHOS, and functions as a sensor of redox changes and master metabolic regulators of mitochondrial homeostasis^[51-52]. The present data show that the stressors of EMF from mobile phones and fructose consumption (EF) jointly reduce the protein expression of SIRT1 in the hypothalamus and liver to inhibit insulin signaling and mitochondrial oxidative phosphorylation, which have been implicated in IR development^[53-54].

The Foxohead box protein 1 (FOXO-1) integrates insulin signaling with mitochondrial function, and is a critical mediator of impaired glucose homeostasis in hep-IR and mitochondrial oxidative stress^[55-57]. In consonance, FOXO-1 expression in EF was reduced in both the hypothalamus and liver, which may have led to the disintegration of communication between the insulin receptor substrate proteins and mitochondrial oxidative function. It may be deduced that reduced FOXO-1, due to impaired deacetylation by SIRT 1, may be responsible for inhibiting the phosphorylation series of IRS1 the PI3K/AKT cascade. The PI3K/AKT pathway is one of the foremost signal transduction pathways that play a regulatory role in insulin sensitivity mediated by AMPK-SIRT1/FOXO-1, and its inhibition may be pivotal in the pathogenesis of IR^[58-60]. It is evident from our present results that the reduced expression of IRS1 and p-PI3K decreased AKT phosphorylation in the hypothalamus and liver of EF to interrupt downstream insulin signaling (PI3K/ AKT pathway). In EF, AKT fails to regulate glycolysis in the hypothalamus and liver or activates

hepatic gluconeogenesis by directly disrupting SIRT 1 mediated FOXO-1/AKT signaling activation.

Several studies have supported the hypothesis that mitochondrial dysfunction is a key pathomechanism linking obesity and T2DM, both of which are characterized by insulin resistance. A decrease in OXPHOS is most frequently associated with an increase in mitochondrial ROS generation, which has been linked to the onset and progression of metabolic changes^[61-62]. Collectively, these results suggest that concomitant exposure to EMF-MPs and fructose consumption in childhood and adolescence decreases the hepatic oxidative phosphorylation capacity in EF in early adulthood. This leads to disturbed hepatic glucose and lipid homeostasis, which is linked to energy balance, particularly ATP production in EF mice.

Generally, the oxidation and reduction of nicotinamide adenine dinucleotide (NAD⁺/NADH) or flavine-adenine dinucleotide (FAD/FADH₂) molecules by different protein complexes (complexes I-IV) generate a proton gradient in the intermembrane space of the organelles, which is used by ATP synthase (complex V) to convert ADP and organic phosphate into ATP^[63]. In EF mice, reduced complex activity, along with increased ROS levels during OXPHOS, primarily in complexes I and III, lead to oxidative stress.

An intrinsic mitochondrial malfunction at the level of the oxidative phosphorylation system and electron transport chain results in mitochondrial dysfunction, which manifests as a primary defect and hinders insulin signaling, causing IR by activating a cascade of events, culminating in the intracellular diacylglycerol accumulation^[64]. It has been hypothesized that a high-fructose diet reduces mitochondrial respiration and ATP generation^[65]. Similarly, exposure to EMFs also affects biological systems by increasing ROS and altering the activities of antioxidant defense enzymes and the OXPHOS system^[66-67].

Our study indicates that the combined effect of EMF-MPs and fructose consumption (15%) reduces OXPHOS (complexes I, II, III, and IV) in the electron transport chain. The transport of electrons generated from the oxidation of NADH and FADH₂ is hindered during glycolysis, and beta-oxidation alters the electrochemical gradient. Furthermore, reduced complex V activity leads to decreased oxidative capacity, mitochondrial dysfunction, and reduced ATP production in EF mice.

UCP2 is an anion carrier expressed in the mitochondrial inner membrane that uncouples

oxygen consumption by the respiratory chain from ATP synthesis and acts as a negative regulator of ROS production in the mitochondrial respiratory chain^[68-69]. Here, we report that in EF, the hypothalamic and hepatic UCP2 expression is decreased compared to that in normal tissue. Our findings showed that in EF mice, the expression of mitochondrial OXPHOS proteins (complexes I, II, III, IV, and ATPase) was reduced, and oxidative stress was increased in the hypothalamus and liver. Moreover, reduced levels of intracellular SOD, catalase, and GSH activity, along with decreased hypothalamic and hepatic mitochondrial MnSOD expression in EF mice indicate that the pathway responsible for mitigating oxidative stress is diminished.

Taken together, these data show that the concomitant effect of EMF-MPs and 15% fructose consumption leads to the development of hypothalamic and hepatic insulin resistance in EF by early adulthood. Central and peripheral master metabolic regulators (AMPK-SIRT1/UCP2-FOXO1), insulin receptor substrate signals (IRS1/PI3K/AKT), and mitochondrial functions (OXPHOS) were severely disrupted. Impaired master metabolic regulators perturb insulin signaling and diminish mitochondrial OXPHOS. This study is clinically relevant as it provides evidence that exposure to EMF-MPs with unrestricted 15% fructose consumption during childhood and adolescence causes IR in adulthood, which may become a major risk factor for the development of NAFLD and metabolic syndrome by early adulthood.

CONCLUSION

These data indicate that the EMF from mobile phones and fructose consumption during childhood-adolescence coalesce to mitigate master metabolic regulators (AMPK-SIRT1) and signals of oxidative phosphorylation and insulin functions (UCP2 and FOXO1) in the hypothalamus and liver, ultimately initiating the genesis of hyp-IR and hep-IR by early adulthood.

AUTHOR CONTRIBUTIONS

Ruchi Tripathi performed the experiments, collected and analyzed the data, and wrote the manuscript; Sanjay K Baneerje supervised the experiment and revised the manuscript; Jay Prakash Nirala designed the automatic exposure chamber system and measured the power density and SAR

value of mobile phones; Rajani Mathur generated the funding, supervised the study, designed the experiment, and wrote and reviewed the manuscript.

CONFLICTS OF INTEREST

The authors declare no conflicts of interest.

Received: November 10, 2022;

Accepted: June 17, 2023

REFERENCES

- Fried M, Yumuk V, Oppert JM, et al. Interdisciplinary European guidelines on metabolic and bariatric surgery. *Obes Facts*, 2013; 6, 449–68.
- Frühbeck G, Toplak H, Woodward E, et al. Obesity: the gateway to ill health—an EASO position statement on a rising public health, clinical and scientific challenge in Europe. *Obes Facts*, 2013; 6, 117–20.
- Kelly T, Yang W, Chen CS, et al. Global burden of obesity in 2005 and projections to 2030. *Int J Obes*, 2008; 32, 1431–7.
- Hossain P, Kawar B, El Nahas M. Obesity and diabetes in the developing world—a growing challenge. *N Engl J Med*, 2007; 356, 213–5.
- Chen WY, Balland E, Cowley MA. Hypothalamic insulin resistance in obesity: effects on glucose homeostasis. *Neuroendocrinology*, 2017; 104, 364–81.
- Das SK, Balakrishnan V. Role of cytokines in the pathogenesis of non-alcoholic fatty liver disease. *Indian J Clin Biochem*, 2011; 26, 202–9.
- Vos MB, Lavine JE. Dietary fructose in nonalcoholic fatty liver disease. *Hepatology*, 2013; 57, 2525–31.
- Perrari I, Buyken AE, Penczynski KJ, et al. Relevance of fructose intake in adolescence for fatty liver indices in young adulthood. *Eur J Nutr*, 2021; 60, 3029–41.
- Mathur R, Sehgal R, Rajora P, et al. *Aegle marmelos* impedes onset of insulin resistance syndrome in rats provided with drinking fructose from weaning to adulthood stages of development—a mechanistic study. *Can J Physiol Pharmacol*, 2017; 95, 572–9.
- Aggarwal H, Nair J, Sharma P, et al. *Aegle marmelos* differentially affects hepatic markers of glycolysis, insulin signalling pathway, hypoxia, and inflammation in HepG2 cells grown in fructose versus glucose-rich environment. *Mol Cell Biochem*, 2018; 438, 1–16.
- Nair J, Velpandian T, Das US, et al. Molecular and metabolic markers of fructose induced hepatic insulin resistance in developing and adult rats are distinct and *Aegle marmelos* is an effective modulator. *Sci Rep*, 2018; 8, 15950.
- Moon JH. Health effects of electromagnetic fields on children. *Clin Exp Pediatr*, 2020; 63, 422–8.
- Challis LJ. Mechanisms for interaction between RF fields and biological tissue. *Bioelectromagnetics*, 2005; 26, S98–S106.
- Wainwright P. Thermal effects of radiation from cellular telephones. *Phys Med Biol*, 2000; 45, 2363–72.
- Wust P, Kortüm B, Strauss U, et al. Non-thermal effects of radiofrequency electromagnetic fields. *Sci Rep*, 2020; 10, 13488.
- Wiedemann P, Schütz H. Children's health and RF EMF exposure. Views from a risk assessment and risk communication perspective. *Wien Med Wochenschr*, 2011; 161, 226–32.
- Dimbylow PJ, Mann SM. SAR calculations in an anatomically realistic model of the head for mobile communication transceivers at 900 MHz and 1.8 GHz. *Phys Med Biol*, 1994; 39, 1537–53.
- Kleinlogel H, Dierks T, Koenig T, et al. Effects of weak mobile phone—electromagnetic fields (GSM, UMTS) on event related potentials and cognitive functions. *Bioelectromagnetics*, 2008; 29, 488–97.
- Al-Khlaiwi T, Meo SA. Association of mobile phone radiation with fatigue, headache, dizziness, tension and sleep disturbance in Saudi population. *Saudi Med J*, 2004; 25, 732–6.
- Meo SA, Al-Drees AM. Mobile phone related-hazards and subjective hearing and vision symptoms in the Saudi population. *Int J Occup Med Environ Health*, 2005; 18, 53–7.
- Yakymenko I, Tsybulin O, Sidorik E, et al. Oxidative mechanisms of biological activity of low-intensity radiofrequency radiation. *Electromagn Biol Med*, 2016; 35, 186–202.
- Tripathi R, Banerjee SK, Nirala JP, et al. Simultaneous exposure to electromagnetic field from mobile phone and unimpeded fructose drinking during pre-, peri-, and post-pubertal stages perturbs the hypothalamic and hepatic regulation of energy homeostasis by early adulthood: experimental evidence. *Environ Sci Pollut Res*, 2022; 29, 7438–51.
- Lowry OH, Rosebrough NJ, Farr AL, et al. Protein measurement with the Folin phenol reagent. *J Biol Chem*, 1951; 193, 265–75.
- Marklund S, Marklund G. Involvement of the superoxide anion radical in the autoxidation of pyrogallol and a convenient assay for superoxide dismutase. *Eur J Biochem*, 1974; 47, 469–74.
- Noeman SA, Hamooda HE, Baalash AA. Biochemical study of oxidative stress markers in the liver, kidney and heart of high fat diet induced obesity in rats. *Diabetol Metab Syndr*, 2011; 3, 17.
- Sinha AK. Colorimetric assay of catalase. *Anal Biochem*, 1972; 47, 389–94.
- Ellman GL. Tissue sulfhydryl groups. *Arch Biochem Biophys*, 1959; 82, 70–7.
- Zheng JB, Ramirez VD. Rapid inhibition of rat brain mitochondrial proton F₀F₁-ATPase activity by estrogens: comparison with Na⁺, K⁺-ATPase of porcine cortex. *Eur J Pharmacol*, 1999; 368, 95–102.
- Bradford MM. A rapid and sensitive method for the quantitation of microgram quantities of protein utilizing the principle of protein-dye binding. *Anal Biochem*, 1976; 72, 248–54.
- Chappell JB, Hansford RG. Preparation of mitochondria from animal tissues and yeasts. In: Birnie GD. *Subcellular Components*. 2nd ed. Butterworth-Heinemann. 1972, 77–91.
- Pollard AK, Craig EL, Chakrabarti L. Mitochondrial complex 1 activity measured by spectrophotometry is reduced across all brain regions in ageing and more specifically in neurodegeneration. *PLoS One*, 2016; 11, e0157405.
- Spinazzi M, Casarin A, Pertegato V, et al. Assessment of mitochondrial respiratory chain enzymatic activities on tissues and cultured cells. *Nat Protoc*, 2012; 7, 1235–46.
- Barrientos A, Fontanesi F, Diaz F. Evaluation of the mitochondrial respiratory chain and oxidative phosphorylation system using polarography and spectrophotometric enzyme assays. *Curr Protoc Hum Genet*, 2009.
- Kramer KA, Oglesbee D, Hartman SJ, et al. Automated spectrophotometric analysis of mitochondrial respiratory chain complex enzyme activities in cultured skin fibroblasts. *Clin Chem*, 2005; 51, 2110–6.

35. Griffiths DE, Houghton RL. Studies on energy-linked reactions: modified mitochondrial ATPase of oligomycin-resistant mutants of *Saccharomyces cerevisiae*. *Eur J Biochem*, 1974; 46, 157–67.
36. Fiske CH, Subbarow Y. The colorimetric determination of phosphorus. *J Biol Chem*, 1925; 66, 375–400.
37. Ono H. Molecular mechanisms of hypothalamic insulin resistance. *Int J Mol Sci*, 2019; 20, 1317.
38. Brown MS, Goldstein JL. Selective versus total insulin resistance: a pathogenic paradox. *Cell Metab*, 2008; 7, 95–6.
39. Meshkani R, Adeli K. Hepatic insulin resistance, metabolic syndrome and cardiovascular disease. *Clin Biochem*, 2009; 42, 1331–46.
40. Ross R, Després JP. Abdominal obesity, insulin resistance, and the metabolic syndrome: contribution of physical activity/exercise. *Obesity*, 2009; 17, S1–2.
41. Reedy J, Krebs-Smith SM. Dietary sources of energy, solid fats, and added sugars among children and adolescents in the United States. *J Am Diet Assoc*, 2010; 110, 1477–84.
42. Elliott SS, Keim NL, Stern JS, et al. Fructose, weight gain, and the insulin resistance syndrome. *Am J Clin Nutr*, 2002; 76, 911–22.
43. Bray GA, Nielsen SJ, Popkin BM. Consumption of high-fructose corn syrup in beverages may play a role in the epidemic of obesity. *Am J Clin Nutr*, 2004; 79, 537–43.
44. Ribeiro A, Igual-Perez MJ, Santos Silva E, et al. Childhood fructoholism and fructoholic liver disease. *Hepato Comm*, 2019; 3, 44–51.
45. Das UN. Obesity: genes, brain, gut, and environment. *Nutrition*, 2010; 26, 459–73.
46. Amitani M, Asakawa A, Amitani H, et al. The role of leptin in the control of insulin-glucose axis. *Front Neurosci*, 2013; 7, 51.
47. Kalra SP. Disruption in the leptin–NPY link underlies the pandemic of diabetes and metabolic syndrome: new therapeutic approaches. *Nutrition*, 2008; 24, 820–6.
48. Dodd GT, Tiganis T. Insulin action in the brain: roles in energy and glucose homeostasis. *J Neuroendocrinol*, 2017; 29, e12513.
49. Garcia D, Shaw RJ. AMPK: mechanisms of cellular energy sensing and restoration of metabolic balance. *Mol Cell*, 2017; 66, 789–800.
50. Miyamoto T, Rho E, Sample V, et al. Compartmentalized AMPK signaling illuminated by genetically encoded molecular sensors and actuators. *Cell Rep*, 2015; 28, 657–70.
51. Aquilano K, Baldelli S, Pagliari B, et al. Extranuclear localization of SIRT1 and PGC-1 α : an insight into possible roles in diseases associated with mitochondrial dysfunction. *Curr Mol Med*, 2013; 13, 140–54.
52. Wan XX, Garg NJ. Sirtuin control of mitochondrial dysfunction, oxidative stress, and inflammation in Chagas disease models. *Front Cell Infect Microbiol*, 2021; 11, 693051.
53. Liang FX, Kume S, Koya D. SIRT1 and insulin resistance. *Nat Rev Endocrinol*, 2009; 5, 367–73.
54. Hori YS, Kuno A, Hosoda R, et al. Regulation of FOXOs and p53 by SIRT1 modulators under oxidative stress. *PLoS One*, 2013; 8, e73875.
55. Ponugoti B, Dong GY, Graves DT. Role of forkhead transcription factors in diabetes-induced oxidative stress. *Exp Diabetes Res*, 2012; 2012, 939751.
56. Cheng ZY, Guo SD, Copps K, et al. Foxo1 integrates insulin signaling with mitochondrial function in the liver. *Nat Med*, 2009; 15, 1307–11.
57. Sin TK, Yung BY, Yip SP, et al. SIRT1-dependent myoprotective effects of resveratrol on muscle injury induced by compression. *Front Physiol*, 2015; 6, 293.
58. Huang XJ, Liu GH, Guo J, et al. The PI3K/AKT pathway in obesity and type 2 diabetes. *Int J Biol Sci*, 2018; 14, 1483–96.
59. Ruderman NB, Xu XJ, Nelson L, et al. AMPK and SIRT1: a long-standing partnership? *Am J Physiol Endocrinol Metab*, 2010; 298, E751–60.
60. Wang RH, Kim HS, Xiao CY, et al. Hepatic *Sirt1* deficiency in mice impairs mTorc2/Akt signaling and results in hyperglycemia, oxidative damage, and insulin resistance. *J Clin Invest*, 2011; 121, 4477–90.
61. Kim JA, Wei YZ, Sowers JR. Role of mitochondrial dysfunction in insulin resistance. *Circ Res*, 2008; 102, 401–14.
62. Pinti MV, Fink GK, Hathaway QA, et al. Mitochondrial dysfunction in type 2 diabetes mellitus: an organ-based analysis. *Am J Physiol Endocrinol Metab*, 2019; 316, E268–85.
63. Zhao RZ, Jiang S, Zhang L, et al. Mitochondrial electron transport chain, ROS generation and uncoupling (Review). *Int J Mol Med*, 2019; 44, 3–15.
64. Chavez JA, Summers SA. A ceramide-centric view of insulin resistance. *Cell Metab*, 2012; 15, 585–94.
65. Emilie C, Corinne MB, Véronique P, et al. Diets high in sugar, fat, and energy induce muscle type-specific adaptations in mitochondrial functions in rats. *J Nutr*, 2006; 136, 2194–200.
66. Kivrak EG, Yurt KK, Kaplan AA, et al. Effects of electromagnetic fields exposure on the antioxidant defense system. *J Microsc Ultrastruct*, 2017; 5, 167–76.
67. Schuermann D, Mevissen M. Manmade electromagnetic fields and oxidative stress-biological effects and consequences for health. *Int J Mol Sci*, 2021; 22, 3772.
68. Andrews ZB. Uncoupling protein-2 and the potential link between metabolism and longevity. *Curr Aging Sci*, 2010; 3, 102–12.
69. Migliaccio V, Scudiero R, Sica R, et al. Oxidative stress and mitochondrial uncoupling protein 2 expression in hepatic steatosis induced by exposure to xenobiotic DDE and high fat diet in male Wistar rats. *PLoS One*, 2019; 14, e0215955.